

CHAPTER 95

WAVE FORCES ON SUBMERGED PIPE LINES

by

Ernest F. Brater¹ and Roger Wallace²

ABSTRACT

This is a presentation of the analyses of data obtained from a laboratory investigation of horizontal forces produced by oscillatory waves on submerged pipes. The research program was planned to help solve design problems for pipe lines located on or below the bottom in the oceans or the Great Lakes. The project was financed by the National Science Foundation.

A continuous record of wave height and horizontal force was obtained for pipes of four diameters, for three wave heights and three wave lengths. Forces were measured at four locations below the water surface, the lowest position being as near the bottom as possible. Other tests were conducted with the pipes located in various positions within trenches of several different shapes. The actual pipe diameters, wave heights and wave periods used in the laboratory tests were such that on the basis of a scale ratio of 1 to 75 the range of prototype parameters would include pipe diameters varying from 8 to 15 feet, wave heights varying from 8 to 23 feet and wave periods in the range from 6 seconds to 12 seconds. Results are presented in the form of coefficients of inertial resistance and drag which can be used with the Airy equations to compute forces.

INTRODUCTION

The increasing use of submerged pipelines for water intakes and sewer outfalls and for the transportation of oil, gas and other chemicals has created considerable interest and concern regarding the magnitudes of design forces. Not only are failures of such pipelines very costly but there is an increasing concern because of the almost irreparable environmental damage that might occur. A review of various aspects of the problem has been presented by Ralston & Herbich (1969). In a summary of the various hazards to submerged pipelines, Ried (1954) has placed wave action at the top of the list. Grace (1971) has summarized previous research on this topic.

1 Professor of Hydraulic Engineering, Department of Civil Engineering, University of Michigan

2 Hydraulic Engineer, Michigan Water Resources Commission

The investigation of forces created by oscillatory waves on submerged structures was started at the University of Michigan Lake Hydraulics Laboratory with tests on a proposed off-shore drilling structure (Brater and Maugh, 1953). The first basic research effort dealt with forces on barge-like shapes (Brater, McNown & Stair, 1961). Interest in a second project dealing with forces on submerged pipelines arose because of the senior author's involvement in re-designing pipelines which had failed due to wave forces. Such failures occurred at depths of from 20 to 40 feet with the pipes exposed in trenches. Estimates of the necessary coefficients could be made from values determined for vertical piling (Morrison, Johnson & O'Brien, 1954). However, because of the uncertainties involved the designs were probably somewhat conservative. The previous experience with research on wave forces indicated that a laboratory testing program would supply the necessary design information. Accordingly, application was made to the National Science Foundation for financial assistance. The grant was made and the research was carried out over a period of five years.

HYDRAULICS OF OSCILLATORY WAVES

The water motion associated with oscillatory waves is one of rotation in nearly closed circular or elliptical orbits. When wave motion is from left to right the orbital motion is clockwise. If one envisions a sinusoidal wave form* as sketched in Fig. 1, then phase angles (θ) can be used to designate points between successive crests. One can either visualize the motion at a point with respect to time (t) or instantaneous conditions at location (x) as indicated in Fig. 1. The time and horizontal space parameters can be combined into the following equations for θ and the water surface profile (y). In these equations L is the wave length and T is the wave period.

$$\theta = 2\pi \left(\frac{x}{L} - \frac{t}{T} \right) \quad (1)$$

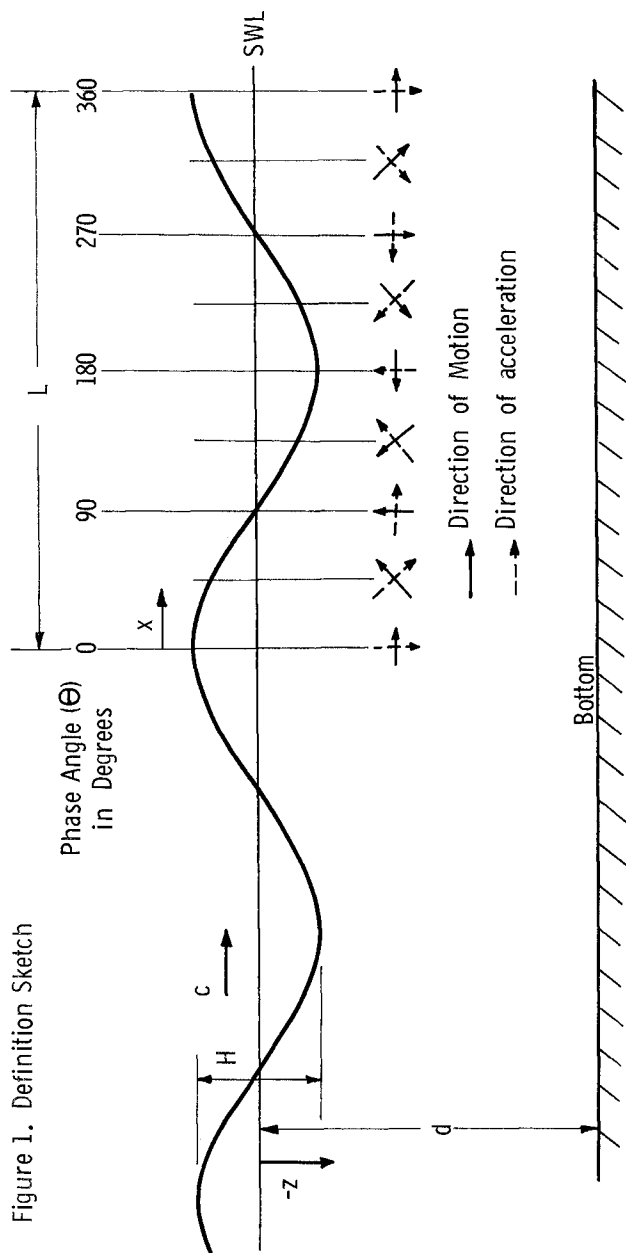
$$y = \frac{H}{2} \cos \theta \quad (2)$$

The corresponding directions of water movement for any phase angle are as depicted by the solid arrows in Fig. 1. The orbital velocities create drag forces on submerged bodies of the form expressed by Eq. (3) in which A is the projected area

$$F_d = C_d \rho A \frac{u^2}{2} \quad (3)$$

on a plane perpendicular to u , C_d is the drag coefficient and ρ is fluid density. It will be seen that drag forces on a fixed body are in the direction of wave motions when a crest

* The water motion will be described and the force equations developed on the basis of the Airy theory. Thereafter some implications of the Stokes theory will be discussed.



is above the body and that the drag force rotates in a clockwise direction thru 360 degrees with the passage of each wave. This variation in direction of the horizontal drag force is expressed analytically in terms of component in the x direction as shown by Equation (4).

$$F_{dx} = C_{dx} \rho A_x \frac{u_x^2}{2} \quad (4)$$

The value of u_x is given by Equation 5.

$$u_x = \frac{\pi H}{T} \frac{\cosh 2\pi (d+z)/L}{\sinh 2\pi d/L} \cos \theta \quad (5)$$

The other type of force produced by the orbital motion is caused by pressure differences and is called the inertial force (King and Brater, 1963). This is the force which would have been required to accelerate the fluid displaced by the solid body plus the additional force due to the flow disturbance caused by the presence of the solid body. This additional force is taken care of by including a coefficient of inertial resistance (C_m) in the expression for this force shown in Eq. (6), in which V is the volume of the submerged body. The

$$F_i = C_m \rho V \frac{\partial u}{\partial t} \quad (6)$$

amount that C_m exceeds unity may be thought of as related to the additional mass of fluid affected by the presence of the body and is sometimes called the coefficient of virtual mass, hence the use of the subscript m in on the coefficient. This force acts in the direction of wave motion for $\theta = 90^\circ$ and, as can be seen by the dotted arrows in Fig. 1, it is 90° out of phase with the drag force. The horizontal component of the inertial force is shown by Eq. 7.

$$F_{ix} = C_{mx} \rho V \frac{\partial u}{\partial t} \quad (7)$$

The value of $\frac{\partial u_x}{\partial t}$ is given by Eq. (8).

$$\frac{\partial u_x}{\partial t} = \frac{2\pi^2 H}{T^2} \frac{\cosh 2\pi (d+z)/L}{\sinh 2\pi d/L} \sin \theta \quad (8)$$

Referring to Equations (4) and (7) and to Fig. 1 it may be seen that both forces have positive components in the x direction for $0 < \theta < 90$ and negative components in the x direction for $180 < \theta < 270$ thus creating the possibility that the maximum horizontal force (F_x) will be a combination

of F_m and F_d at intermediate phase angles. The expression for F_x is

$$F_x = F_{dx} + F_{ix} \quad (9)$$

Differentiation of F_x with respect to θ and setting the result equal to zero yields the following expression for the angle of maximum combined force.

$$\sin \theta_{\max} = \frac{2C_m V \sinh 2\pi d/L}{C_d A_x H \cosh 2\pi (d+z)/L} \quad (10)$$

One difficulty in dealing with Eqs. (4), (5), and (7) and (8) is that values of u and $\partial u/\partial t$ vary from point to point and therefore in estimating forces on submerged bodies a weighted average value of u and $\partial u/\partial t$ should be used. For the case of inertial forces on very large structures this problem has been solved conveniently by writing Eq. (7) in terms of pressure differences (Brater, McNown & Stair, 1962). For most pipelines the size of the structure is so small compared to stormwave lengths that the weighted average differs little from the value at the center of the body.

Perhaps the most troublesome decision that must be made in developing an analytical basis for computing wave forces is the choice of the theory to be used for computing u and $\partial u/\partial t$. The Airy equations which have been used in this discussion have the tremendous advantage of simplicity. Even though tables (Skjelbreia, 1958) have been developed which make it much easier to use the Stokes equations it would require a great improvement in accuracy to warrant the expenditure of the additional time. Actually the differences between computed values of orbital velocity and acceleration are small.

From the point of view of finding an adequate analytical approach for computing maximum wave forces the most important difference between the Airy and Stokes theories is the difference in the phase angles of the maximum acceleration. According to the Airy theory these phase angles (θ_m) are 90 and 270 degrees. Within the range of H , L and d for these tests, values of θ_m computed from the Stokes equations (Skjelbreia, 1958) are also 90° for downwave acceleration for $L = 2.6$ feet but for $L = 4.1$ feet θ_m varies from 86 to 88 degrees and for $L = 6.7$, θ_m varies from 72 to 83 degrees. This would mean that for large values of L a measured value of θ_m as small as 72 degrees might indicate that the maximum force is entirely of the inertial type and that F_d is negligible. This point becomes academic however, when one considers Eq.'s (4), (5), (7) and (8) for the case where θ is 72°. The value of $\sin 72^\circ$ is 0.95 and that of $\cos^2 72^\circ$ is 0.10. Therefore for

phase angles of 72° the Airy theory would give practically the same answer whether the forces were computed from Eq. (9) including both types of forces or from Eq. (7) with $\sin \theta = 1$.

EXPERIMENTAL PROCEDURE

Waves were generated by a plunger type wave machine located near one end of a tank 93 feet long and 14 feet wide. The wave machine was capable of generating waves with heights as large as 0.35 feet and with periods as short as 0.7 seconds. A mat of plastic hair was placed behind the wave machine as well as at the opposite end of the tank to dampen reflections. Although this material is very efficient very small reflections were returned from the far end of the tank but in all cases the test run was completed before those reflections returned to the dynamometer.

The test specimen was suspended from a dynamometer located about 40 feet from the wave generator. The test specimens were 4.5 feet long. Additional pipe of the same diameter was mounted at either end of the test specimen so that the pipe extended for the full width of the wave tank except for the small gap between the test specimen and the dummy end sections. Horizontal forces exerted on the test specimens were transmitted to vertical cantilever beams upon which strain gages were mounted. The signals from the strain gages were amplified and recorded with a pen recorder. The dynamometer was calibrated for both up-wave and down-wave forces. The relation was nearly linear and varied little from one test to the next but was re-checked frequently during tests.

Wave heights were measured by a resistance gage located about six feet in front of the dynamometer and on the center line of the tank. The gage was calibrated by raising it and lowering it known amounts, within the tank at its permanent location. The calibration changed very little but was checked frequently. Its output was recorded by pen on an oscillograph chart. A hook gage mounted on the same truss as the wave gage was used to check the water surface elevation in the tank. The time relation of horizontal forces to wave form was determined by mounting a second wave gage above the center of the test specimen. The output from this gage was recorded on the same chart as the wave force trace.

The wave period was determined from the wave trace knowing the rate of movement of the chart paper. Wave lengths were then computed from the periods. It was also necessary to run force tests to determine the corrections for the forces on the portion of the dynamometer which extended below the water surface. Even though this portion of the dynamometer was slender the forces were sufficient to require a small correction particularly when the specimen was located near or below the bottom. Several experimental difficulties were

encountered in conducting these tests. Fully 80 per cent of the time was spent in eliminating problems which affected the quality of the results. The most difficult problem was that of extraneous input to the force recorder. This was solved only after the measurement of vertical forces was abandoned and an electronic filter was installed in the system.

EXPERIMENTAL PROGRAM

A continuous record of wave height and horizontal force was obtained for pipes of four diameters, for three wave heights and three wave lengths. For each set of test parameters forces were measured at four locations ($-z$) below the water surface, the lowest position being as near the bottom as possible. Other tests were made with pipes placed in various locations in trenches of several different shapes. The water depth was kept at one foot at all times. Numerical values of the parameters are shown in Table 1.

TABLE 1
TEST PARAMETERS

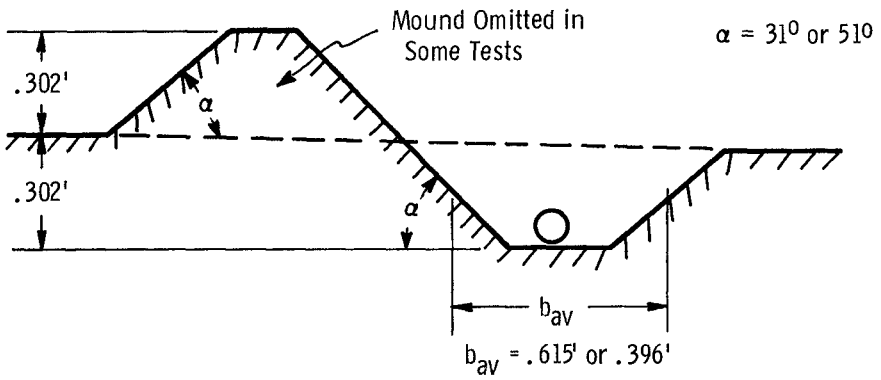
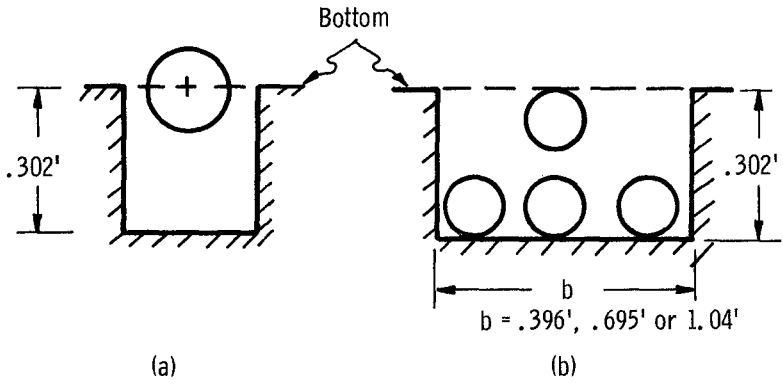
Pipe Diameters (D) in ft.	0.104	0.140	0.159	0.198		
Wave Heights ⁽¹⁾ (H) in ft.	0.11	0.21	0.31			
Wave Lengths ⁽¹⁾ (L) in ft.	6.1	4.1	2.6			
Distances Below						
Water Surface ⁽¹⁾ ($-z/d$)	0.25	0.50	0.75	0.96 ⁽²⁾	1.2 ⁽³⁾	

- (1) These are typical values for each group. Individual values varied slightly.
 (2) Pipe very near the bottom.
 (3) Pipe in a trench.

The only conditions in this array that were not tested were the cases of the largest wave height (.31') combined with the shortest wave length (2.6') which resulted in waves which were very steep and unstable. The ranges of the ratios of wave height, depth and pipe diameter to the wave length were $.016 < H/L < .081$, $.149 < d/L < .385$ and $.016 < D/L < .076$ respectively.

The tests conditions for pipes located in trenches are illustrated in Fig. 2. The condition shown in Fig. 2a simulates a pipe half burried in the bottom. Figures 2b and 2c show conditions which are similar to those that might exist in an open trench. The various circles in Fig. 2(b)

Figure 2. Types of Trenches



(c)

show the locations at which the pipe was placed. With the pipes in a trench, a full range of wave parameters was tested only for a pipe diameter of 0.159 feet but a limited number of parameters were studied for the other three diameters.

ANALYSIS OF RESULTS

Phase Angles of Maximum Forces. The phase angles (θ_p) at which the positive or the down-wave forces are a maximum would be expected to occur in the range from 0 to 90 degrees based on the Airy theory and phase angles at the maximum negative or up-wave forces (θ_n) in the range from 180 to 270 degrees. This is illustrated in Figure 3 which shows computed values of F_d and F_i as well as measured and computed values of (F_d+F_i) for conditions from Test 83. The measured value θ_p and θ_n were 63° and 250° respectively. In the interest of simplicity, only θ_p will be used in this discussion. Average measured values of θ_p for the various diameters varied from 65° for the smallest diameter to 77° for the largest.

It was found that the dimensionless number, D^2/HL , is a useful parameter in deciding whether θ_p or θ_n would differ substantially from the phase angle of the maximum inertial force. Values of θ_p are plotted against D^2/HL in Fig. 4. This criterion is not the complete answer because as shown by the symbols one can detect slightly different trends for different pipe diameters. Yet, the relation is good enough to indicate for example that when $D^2/HL < 0.025$, θ_p may be less than 65° and the drag force should be included in the computations for the maximum force.

Coefficients of Inertial Resistance. Because the inertial force as given by Eq. (6) is usually the predominant force, values of the coefficient of inertial resistance (C_m) were considered as the most important contribution of the research program. Values computed from Eq. (7) from the average forces at $\theta = 90^\circ$ and 270° were called C_M . These values might be considered the true values of C_m except that it has been shown in the previous discussions that the maximum positive acceleration probably occurs at an angle somewhat smaller than 90° in many cases.

Another set of values of C_m was computed from Eq. (7) using the average of the maximum positive and negative forces. These were called C_{MM} . The positive forces were sometimes greater and sometimes less than the maximum negative forces. The differences of the averages of the maximum positive or maximum negative forces from the average for both directions varied from 3.3 per cent for the smallest pipe diameter to 1.6 per cent for the largest diameter. In all cases the average of the

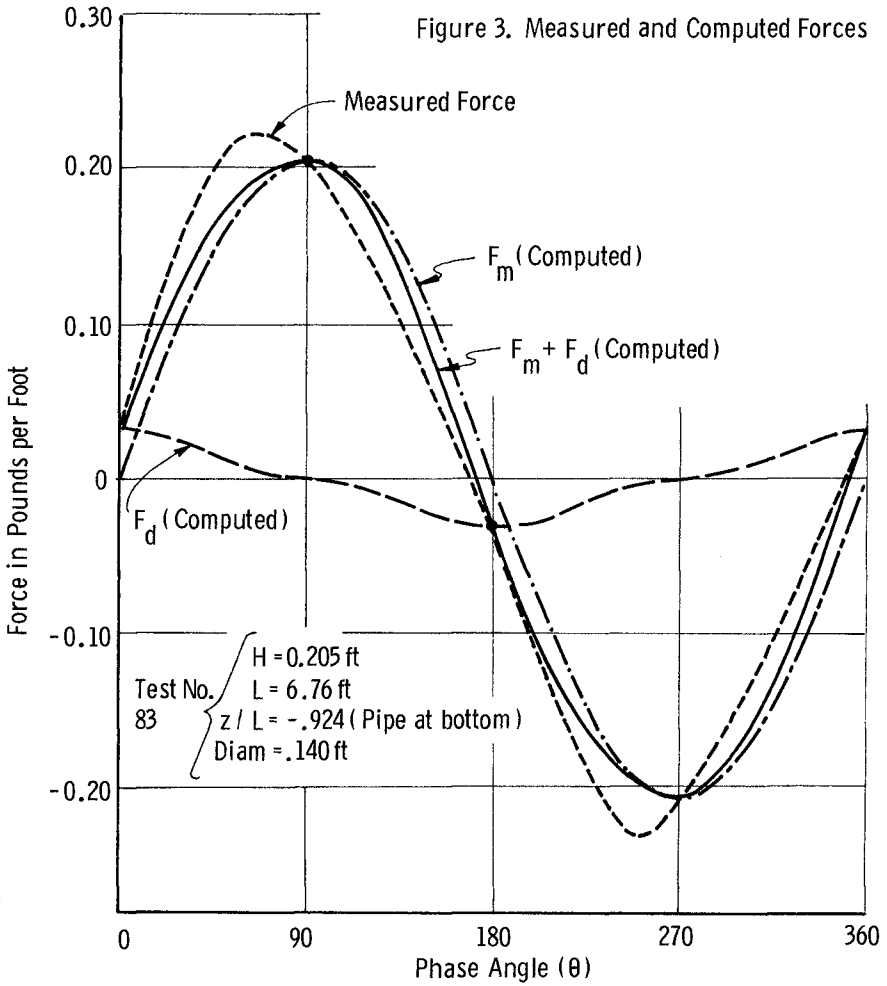
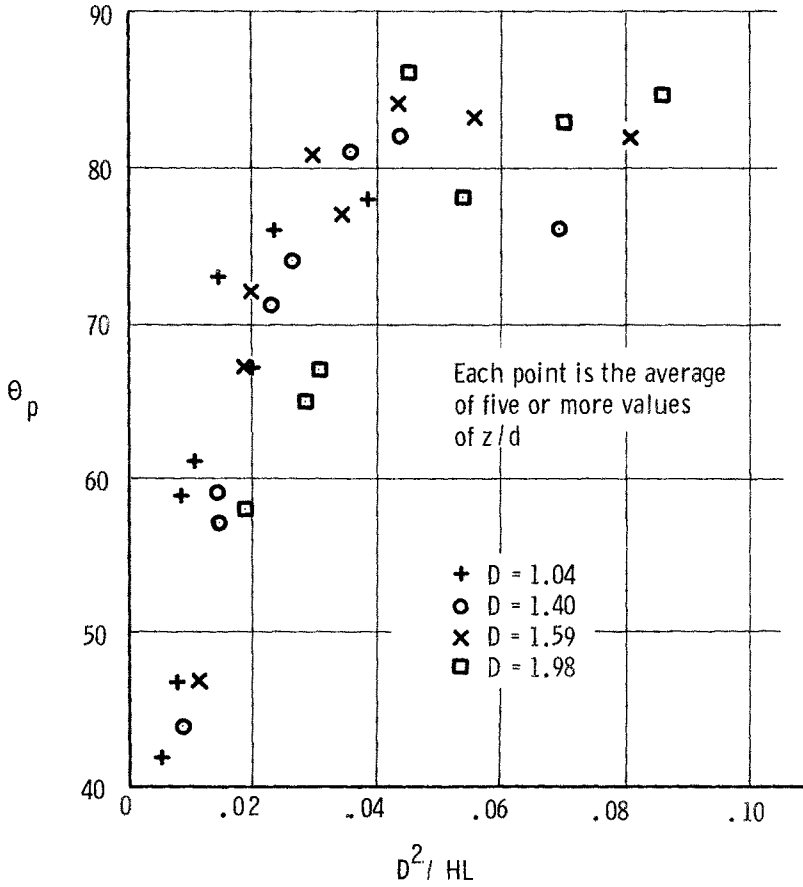


Figure 4. Phase Angles of Maximum Positive Forces



negative forces was greater than the average of the positive forces. The values of CMM could be used to estimate the average total force, assuming the drag force to be negligible.

Another set of values of C_m was derived from the maximum forces obtained from each test and irregardless of the direction of the force. These coefficients were designated as CMMM. They might be used for conservative estimates of the maximum forces assuming the drag forces to be negligible.

In considering various ways of presenting the derived values of C_m it was found that values were relatively independent of D and H but varied in a very orderly linear manner with z/L . Therefore this method of presenting the data was selected. A computer program was written to determine the optimized least square fit for the points in various categories. The values determined were the slope (m), the intercept (b), the linear correlation coefficient (r) and the standard deviation from the regression (S_r). The first six lines of Table 2 give the coefficients for three locations above the bottom. The four pipe diameters were analyzed separately, then all diameters together and finally all diameters except the smallest ($D = 0.104$). In all cases all three wave heights are included in each category. The next category includes all diameters and wave heights with the pipe very near the bottom (line 7, Table 2). Values of z/d differ somewhat for this category because of the differences in pipe diameters, z being the distance from the water surface to the center of the pipe. Therefore -0.9 is a nominal value of z/d . The final category, for which coefficients are given in line 8, represents a half buried pipe for all diameters and wave heights.

The linear correlation coefficients (r) are measures of the likelihood that the sets of points should be represented by the least squares linear equation. Values of r_1 shown in the table represent one per cent confidence limits which suggest the value of r for which the likelihood that it could be achieved accidentally is only 1 in 100. Since the values of r for these tests are all very much larger than values of r_1 one must conclude that it is no accident that the groups of values of C_m and $-z/L$ are fitted by straight lines. The values of S_r shown in Table 2 are for the equations representing CMM. The values of S_r for CM and CMMM were very similar in magnitude.

In the categories for $0.25 < -z/d < 0.75$ for the four diameters there are 12 equations (lines 1 thru 4 in Table 2) representing four pipe diameters and three ways of computing C_m . If one were to plot all of these they would, with two exceptions fall very near together. The two exceptions are CMM and CMMM for the smallest pipe diameter (0.104).

Table 2
CORRELATIONS OF C_m WITH z/L

D (Ft)	z/d	CM				CMM				CMMM							
		b	m	r	r_L	b	m	r	r_L	b	m	r	r_L	Eq. NO.			
.198		1.37	6.56	11	0.88	0.39	1.59	5.82	12	0.87	0.39	1.79	5.33	13	0.81	0.39	0.26
.159		1.41	6.36	14	0.83	0.46	1.69	5.41	15	0.79	0.46	1.91	4.96	16	0.72	0.46	0.33
.140	0.75	1.26	5.87	17	0.86	0.48	1.56	5.50	18	0.84	0.48	1.75	5.22	19	0.81	0.48	0.26
.104		1.49	6.65	20	0.90	0.49	2.04	5.32	21	0.82	0.49	2.38	4.84	22	0.72	0.49	0.26
All	0.25	1.38	6.36	23	0.85	0.23	1.73	5.37	24	0.79	0.23	1.97	4.87	25	0.69	0.23	0.32
All except .104	0.25	1.34	6.41	26	0.85	0.25	1.61	5.64	27	0.84	0.25	1.81	5.22	28	0.78	0.25	0.29
All	-0.9	2.59	4.83	29	0.63	0.37	3.07	4.13	30	0.57	0.37	3.20	4.16	31	0.57	0.37	0.52
All	-1.0	0.83	3.11	32	0.74	0.42	1.01	2.85	33	0.70	0.42	1.14	2.78	34	0.60	0.42	0.25

m and b are coefficients in the equation $C_m = b + m (-z/L)$
r is the linear correlation coefficient
 r_L is the value of r for a one per cent confidence limit
 S_r is the standard deviation from the regression
CM, CMM and CMMM are values of C_m derived as described in the text.

This is to be expected because as shown in the previous section it is only for the smallest sizes that drag forces tend to make an important contribution to the maximum total forces. It might be concluded that the following equations (line 6 of Table 2) for all values of D except $D = .104'$ may be used when $D^2/HL < .02$.

$$CM = 1.34 + 6.41 (-z/L) \quad (26)$$

$$CMM = 1.61 + 5.64 (-z/L) \quad (27)$$

$$CMMM = 1.81 + 5.22 (-z/L) \quad (28)$$

For small sizes, where $D^2/HL < .02$, it would be better to use the Equations (20), (21) and (22) (line 4 of Table 2) derived for the smallest diameter, $D = 0.104'$. It may be questioned whether such refinements are desirable or necessary because the differences among the various equations are probably very small compared with uncertainties in the selection of a design wave. It would be quite appropriate for design purposes to use Equations (23), (24) and (25) (line 5 of Table 3) derived for all diameters irregardless of any size criterion.

The equations for the pipe on the bottom ($z/d = -0.9$) have excellent correlation coefficients. The standard deviations from the regressions are somewhat larger than for the other equations. These equations have much practical importance because they provide design values for the most vulnerable position in which a pipe can be placed. The equation numbers and coefficients are presented in line 7 of Table 2.

Equations (32), (33) and (34) (line 8, Table 2) give values of C_m for the case of a half buried pipe ($z/d = -1.0$). It should be noted that in computing values of C_m from the test data by means of Eq. (7) the volume was taken as the entire volume of the pipe. Forces computed in this same manner would include the assumption that pressure differences would penetrate the bed material at least to the bottom of the half buried pipe.

The equations for C_m which apply when the pipes are located in trenches of various shapes were not computed by means of a least squares procedure because most of the data were obtained for z/L of about -0.29 (32 tests). A smaller number of values were obtained for a z/L of approximately $-.19$ (six tests) and $z/L = -.47$ (four tests). It was assumed that the relationship would be similar to the ones obtained for the other eight categories. Therefore the large number of tests for a z/L of about -0.29 , for which the average value of CMM was 1.42 , was used to determine the location of the line. The less well defined values for $z/L = -.19$ and $-.47$ respectively were used to determine the slope. In this manner the following equation was derived for pipes in a trench.

$$CMM = 1.0 + 1.4 (-z/L) \quad (35)$$

The values of CM and CMM appears to be smaller and larger than CMM respectively in about the same proportions as for all of the other categories. It did not seem to be worthwhile to try and distinguish differences between coefficients for various shapes of trench or positions of the pipes within the trench. It appeared that when the width of the trench was about 7 times the pipe diameter that conditions were approaching those without a trench.

In order to provide a visual presentation of the relation of the relationships for various conditions all of the Equations for CMM are plotted in Figure 5.

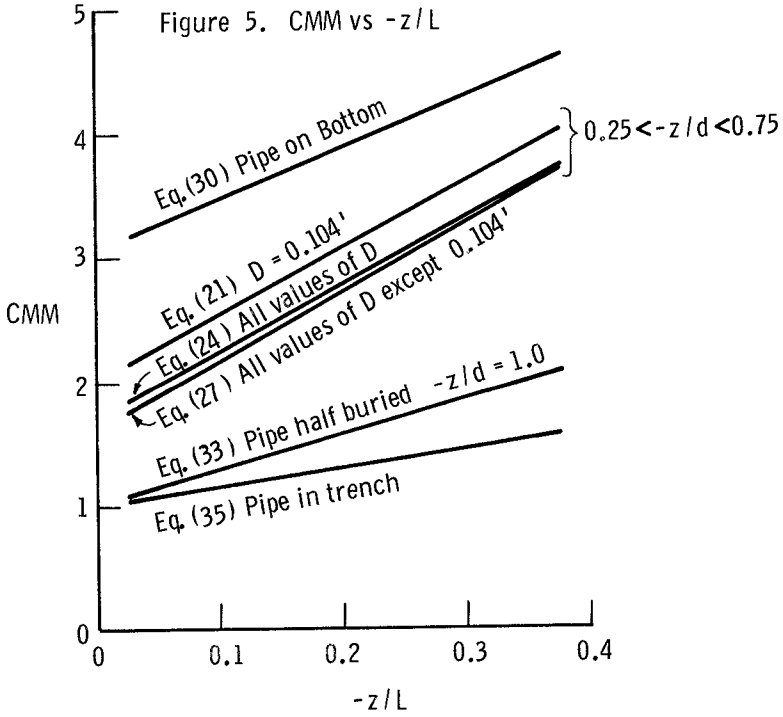
Drag Coefficients. It has been shown in the previous sections that the drag forces play a much less important role in determining the total maximum horizontal forces than do the inertial forces. However, there are situations in which the quantity D^2/HL is very small (less than 0.02) in which it may be desirable or necessary to include the drag force. The drag coefficients were plotted against the Reynolds number (R) which was defined as shown by Eq. (36) in which D is the pipe diameter, u is the orbital

$$R = \frac{Du}{\nu} \quad (36)$$

velocity and ν the kinematic viscosity. The plotted points showed definite trends but were widely scattered. It should be recalled that the drag coefficients were determined from forces at phase angles of 0 to 180 degrees. Since the forces were relatively small at these phase angles and also changing rapidly it might be expected that measured forces might have errors that are larger than in the measured values of the maximum or near maximum forces. It was found that for the range of z/L from -0.25 to -0.75 the points needed to be plotted separately for different values of d/L , but that for each value of d/L the full range of wave heights and pipe diameters could be included. An example is shown in Fig. 6 in which the plotted points are for a nominal value of d/L of 0.24. The solid line was plotted thru these by judgement. On the same graph are also shown the lines but not the points obtained in the same manner for nominal values of d/L of 0.16 and 0.38.

For the case of the pipe on the bottom the values of C_d for all values of d/L were plotted together as shown in Fig. 7. Symbols were used which identify the values of D and d/L for each point. The line representing these points was drawn by judgement.

A similar plotting for the case where the pipe is half burried ($z/d = -1$) is shown in Figure 8. These groups of points included all values of d/L . In all cases the value of A_x in Eq. (6) was taken as the entire area of the pipe and values of R were always computed using the full diameter. This creates an anomaly for the half burried pipe. One can either use the total pipe area as was done here or use only the exposed area



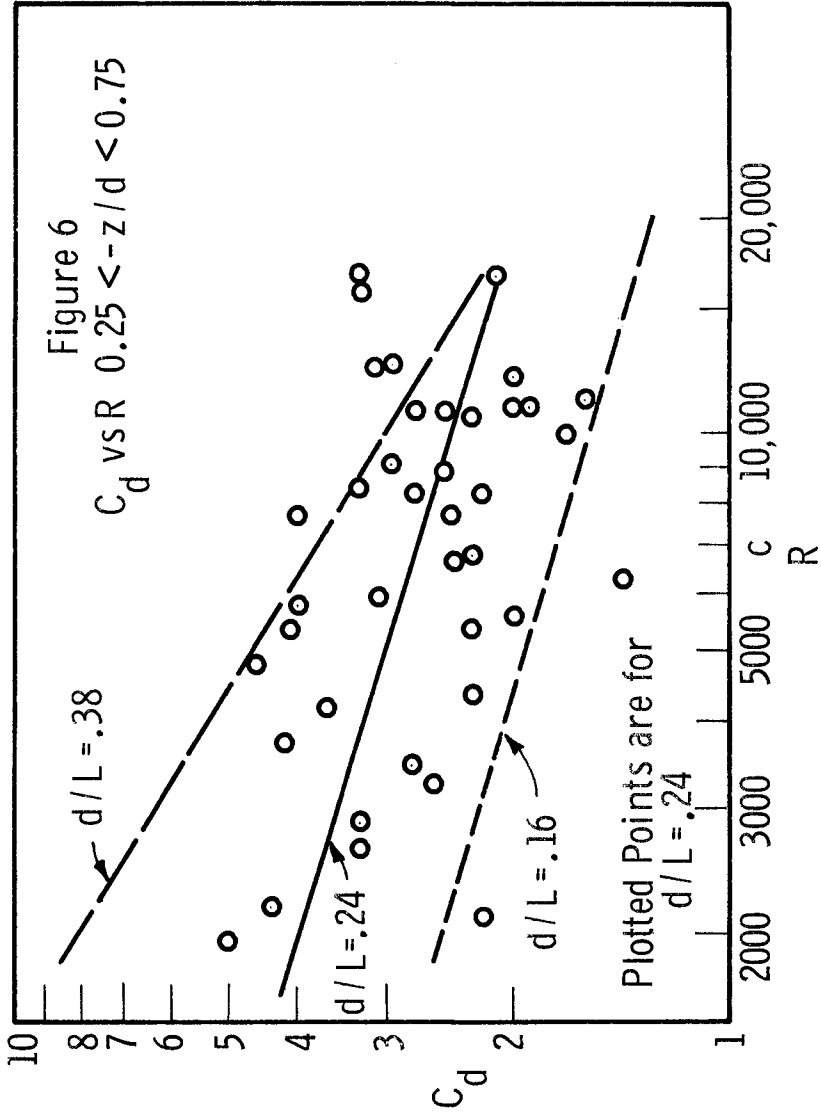
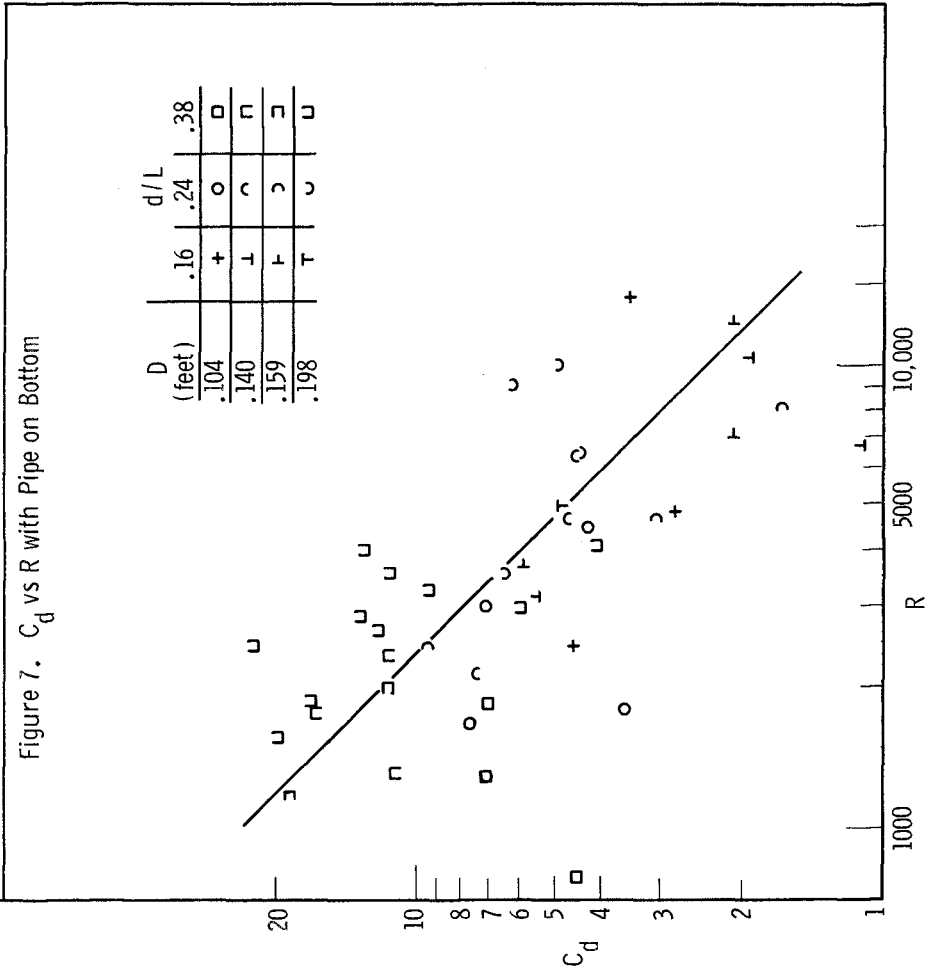


Figure 7. C_d vs R with Pipe on Bottom



and double the values of C_d . Similar lines, but not the points, representing values of C_d for the pipe located in a trench are also shown in Fig. 8.

SUMMARY AND APPLICATIONS

Coefficients of inertial resistance for use in Eqs. (7) or (9) and drag coefficients to be used in Eqs. (4) or (9) were derived for a wide range of pipe diameters, wave heights, wave lengths and pipe locations. Results were plotted against dimensionless parameters which make them suitable for use in practical design problems. The tests showed that the inertial force as given by Eq. (7) predominated but that in the smallest pipe size tested the drag forces were producing noticeable contributions. This could be recognized by the deviation of the phase angles of the maximum forces from those of the maximum inertial forces. The parameter D^2/HL was used to indicate the type of force which is active. When $D^2/HL < 0.02$ the drag forces became important. The coefficients of inertial resistance computed from the average of the maximum positive and negative forces (CMM) or those computed from the maximum force (CMMM) are the most usefull for practical applications. In the range covered by these tests either CMM or CMMM could be used with Eq. (7) to estimate design forces without including a component of the drag force.

REFERENCES

1. Brater, E. F. and L. C. Maugh, "Model Study of an Offshore Drilling Structure," Tech Rept. No. 6, Lake Hydraulics Lab, Dept. of Civil Eng., University of Michigan, 1953.
2. Brater, E. F., John S. McNown and L. D. Stair, "Wave Forces in Submerged Structures," Trans. ASCE, Vol. 126, 1961.
3. Grace, R. L., "Submarine Pipeline Design Against Wave Action," LookLab/Hawaii, Univ. of Hawaii, Vol. 2, No. 2, 1971.
4. King, H. W. and E. F. Brater, "Handbook of Hydraulics," McGraw-Hill Book Co., Inc. 1963, pp. 10-44 to 10-51.
5. Morrison, J. R., J. W. Johnson and M. P. O'Brien, "Experimental Study of Forces on Piles," Proc. 4th Conf. on Coastal Eng., Engineering Foundation, 1954.
6. Ralston, Derwood O., and John B. Herbich, "The Effects of Waves and Currents on Submerged Pipelines," Sea Grant Publ. No. 101, Texas A. & M. University, 1969.
7. Ried, R. O., "Oceanographic Consideration in Marine Pipeline Construction," Contributions in Oceanography and Meteorology, Texas A. & M. University, No. 3, 1950-54.
8. Skjelbreia, Lars, "Gravity Waves, Stokes Third Order Approximation, Table of Functions," Council on Wave Research, Engineering Foundation, 1958.

